



# Multifocal Intraocular Lenses: Basic Principles

# 3

Vicente J. Camps, Juan J. Miret, María T. Caballero,  
David P. Piñero, and Celia García

## 3.1 Introduction

Multifocal intraocular lenses (hereafter, MIOLs) are becoming an effective treatment for cataracts because they are providing good visual quality at different distances. Particularly, in highly developed societies, cataract surgery outcomes are more than just a visual restoration and aim to improve the patient's quality of life by achieving spectacle independence at all distances. Tasks as reading, computer usage, or sport activities can improve very much by spectacle independence.

MIOLs provide simultaneous foci, and the images of objects located at different distances are superimposed on the retina. Therefore, it is necessary to activate the process of neuroadaptation [1].

The main challenge for multifocal lenses is to provide good optical image quality for different object planes, and this is the reason explaining the development of several technologies and designs have been appearing during last years [2].

Basically, MIOLs can be made using refractive and diffractive surfaces or combinations of both. Depending on the optical design, the MIOLs can provide two or three foci. These IOLs can be called bifocal or trifocal lenses, respectively. Bifocal IOLs provide foci for far and near distances and trifocal lenses add a focus for intermediate distances. Furthermore, the proper use of some aberrations or the use of the pinhole effect can increase the depth of focus to provide better intermediate and near distance vision.

Compared with the monofocal IOLs, MIOLs will always provide poorer quality of vision. Halos, glare, reduced contrast sensitivity or reduced retinal illumination are relatively common side effects of MIOLs. Halos will depend on the intensity and size of the out-of-focus image (or images) corresponding to the other foci produced by the lens, which turns out to depend on both add power and energy distribution of the IOL among the foci [3]. In addition, the centering and positioning of these lenses is a critical point and even more when aberrations are used in their designs. Generally, all types of IOLs (including MIOLs) will provide chromatic aberration due to the dependency of the refraction index of the material on the wavelength [4, 5]. In spite of

---

The authors have no proprietary or commercial interest in the medical devices that are involved in this manuscript. The author David P Piñero has been supported by the Ministry of Economy, Industry and Competitiveness of Spain within the program Ramón y Cajal, RYC-2016-20471.

V. J. Camps (✉) · D. P. Piñero  
Grupo de Óptica y Percepción Visual (GOPV),  
Department of Optics, Pharmacology and Anatomy,  
University of Alicante, Alicante, Spain  
e-mail: [vicente.camps@ua.es](mailto:vicente.camps@ua.es)

J. J. Miret · M. T. Caballero · C. García  
Department of Optics, Pharmacology and Anatomy,  
University of Alicante, Alicante, Spain

some designs that have been proposed to eliminate the chromatic aberration [6], the usefulness and effectiveness of these designs is not clear given that the human eye processes the chromatic aberration produced by both the cornea and the lens and possibly the consequences of its elimination may be not beneficial.

An important concept that leads to confusion in MIOLs is the difference between light transmission and light distribution. These are two related concepts but with different meanings. Light transmission is the amount of light that goes through the MIOL and depends on the transmission coefficient. Coefficient transmission ( $\tau$ ) is calculated as the quotient between the emerging ( $E_e$ ) and incoming ( $E_i$ ) energy light,

that is:  $\tau = \frac{E_e}{E_i}$ . This coefficient has no units and

ranges between 0 and 1. A value of 1 indicates that 100% of the light that is incoming to the lens is emerging. This transmission coefficient basically depends on the material that IOLs are made. Nowadays, these materials are very transparent and  $\tau$  is near to 1 independently if the MIOL is refractive or diffractive. Therefore, the light transmission is not expected to produce differences between these two types of MIOLs. The amount of incoming light that reaches the MIOL also depends on the pupil size independently if the MIOL has diffractive or refractive optics. The higher the pupil size is, the higher amount of light goes through ( $E_e$ ) the MIOL and vice versa. As it is well known, the pupil diameter changes in response to different illumination levels as well as with the accommodative reflex and this behav-

ior will determine the emerging light in each moment. On the other hand, an important question is how the emerging light is distributed in different foci. This distribution will be different depending on whether the MIOL is refractive or diffractive, as discussed in the following sections.

MIOLs are today useful and provide good visual results. The lenses currently available in the market provide a large range of solutions and a variety of possibilities to tackle various clinical situations. Although not perfect, today's existing MIOLs do provide, in most of the cases, a satisfactory solution for obtaining good vision at different distances [2]. A good knowledge of the optical basis of MIOLs will help to understand and clarify the behavior and limitations of the MIOLs, and this would allow selecting the most suitable patient for each MIOL. Throughout this chapter, the most important optical and physical fundamentals of the MIOLs will be introduced to better understand how the MIOLs work.

### 3.2 Multifocal Refractive Intraocular Lenses

Multifocal refractive lenses have different refractive zones in the same surface that produce multiple powers. Following this principle of design, bifocal, trifocal, or multifocal refractive MIOLs could be obtained. For instance, bifocal lenses could be achieved by using two separated zones, either using an annular structure or a semicircle structure (Fig. 3.1). The same dividing technology is achieved in trifocal and multifocal refractive lenses.

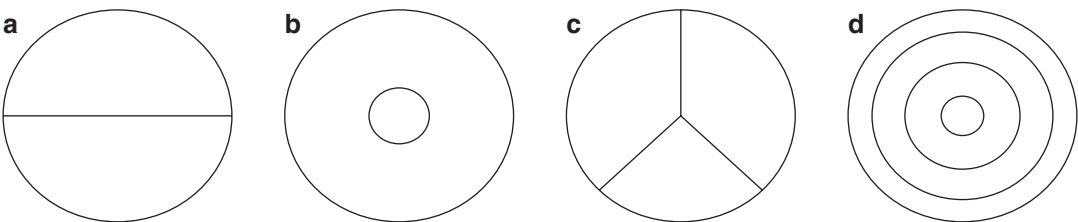


**Fig. 3.1** Schematics of possible configurations for multifocal lenses: (a) simplistic split bifocal, (b) bullet bifocal, (c) triangulate trifocal, and (d) multiple rings [7]

Figure 3.1a corresponds to a semicircle split bifocal design used nowadays in the Mplus family from Oculentis and Lenstec SBL-3 from Lenstec. In this design, the inferior segment provides near vision; meanwhile, the upper segment is intended for far vision. The introduction of more segments allows more possibilities of designs but the orientation and optical properties of angularly segmented multifocal IOLs will determine their optical characteristics<sup>8</sup>.

Using annular ring designs (Fig. 3.1b, d) different types of multifocality could be achieved. For instance, if two rings are used, the central one could provide near vision and the peripheral one far vision, or vice versa. The use of more rings could provide more than two foci for achieving intermediate vision or simply to change the properties of the bifocal design. A trifocal lens could be obtained if the inner zone provides near vision, the middle ring distance vision, and the peripheral outer zone intermediate vision. Different circular or annular refractive MIOLs have been designed over the last decades with two zones (Iolab NuVue), three zones (Storz Tru Vista, Alcon AcuraSee, Ioptex, Morcher, Pharmacia), five zones (AMO Array), or seven zones (Adatomed) [8].

In the refractive MIOLs, the focal distance of each of the foci will be determined by the refraction laws and the local surface curvature of the lens. Therefore, the optical quality of these MIOLs will be different depending on the number of refractive zones, its size, and its location. A critical point in this MIOLs is the transition between the different refractive regions because they can produce straylight effects or generate undesired aberrations [9, 10]. These drawbacks will lead to a loss of contrast sensibility and poorer quality of vision. Another key point in the implantation of these MIOLs will be the tilt and decentering because they may increase these drawbacks [11].

The energy distribution of a refractive MIOL will only depend on its area. For example, assuming a symmetric refractive IOL of radius  $r$ , the emerging energy ( $E_e$ ) will be proportional to the area of this circle, that is,  $E_e \propto \pi r^2$ . A hypothetical bifocal refractive IOL as that shown in Fig. 3.1b

could be made using one central circle of 24 D for near vision and an external ring of 20 D for far vision. Supposing an optical diameter of 6 mm (i.e., a radius  $r_2$  of 3 mm) and a radius of the central circle of  $r_1$  mm, the emerging energy or light that will reach the near focus ( $E_{en}$ ) will be proportional to  $(\pi r_1^2)^2$  and for the far focus ( $E_{ef}$ ) to  $(\pi r_2^2 - \pi r_1^2)^2$ . In refractive MIOLs the eye pupil

size will determine the area of the lens that will transmit light and the light distribution in each focus. A useful radius of the lens ( $r_u$ ) corresponding to the radius of the area of the lens that is being illuminated can be defined. For instance, considering a refractive MIOL 20 D with an addition of 4 D and an optical diameter of 6 mm (that is a radius  $r_2$  of 3 mm), the value of  $r_1$  must be 2.12 mm for obtaining an equivalent light distribution for both foci (that is 50%). Assuming this design, only when the eye pupil size is 6 mm ( $r_u = 3$  mm), the emerging light distribution will be 50% for each focus (Fig. 3.2a, c). For lower eye pupil sizes (for instance  $r_u = 2.5$  mm), the emerging light will be lower and the percentage of light in each focus will be different (see Fig. 3.2b, d). In the case of a pupil size of 4.24 mm ( $r_u = 2.12$  mm), only the zone corresponding to the near vision is illuminated and the 50% of the incoming light is lost. So, the refractive MIOLs will behave as a monofocal IOL producing only a near focus.

Another important aspect is how the light in each focus is distributed. In refractive MIOLs, the width of the focus ( $\Delta$ ) depends inversely on the useful area. As shown in Fig. 3.2c, d, the width of the near and far focus will depend on

$$\frac{1}{\pi r_1^2} \text{ and } \frac{1}{\pi r_u^2 - \pi r_1^2}, \text{ respectively. In Fig. 3.2c,}$$

a pupil size of 6 mm is considered, and two peaks (near and far) have the same amount of light (50%) and same width. In Fig. 3.2d, the pupil size is 5 mm, and it can be observed how the peak of the far focus is lower and wider than the near focus. This effect could be interpreted as a loss in contrast sensibility but also as greater depth of focus. Obviously, this design of bifocal refractive

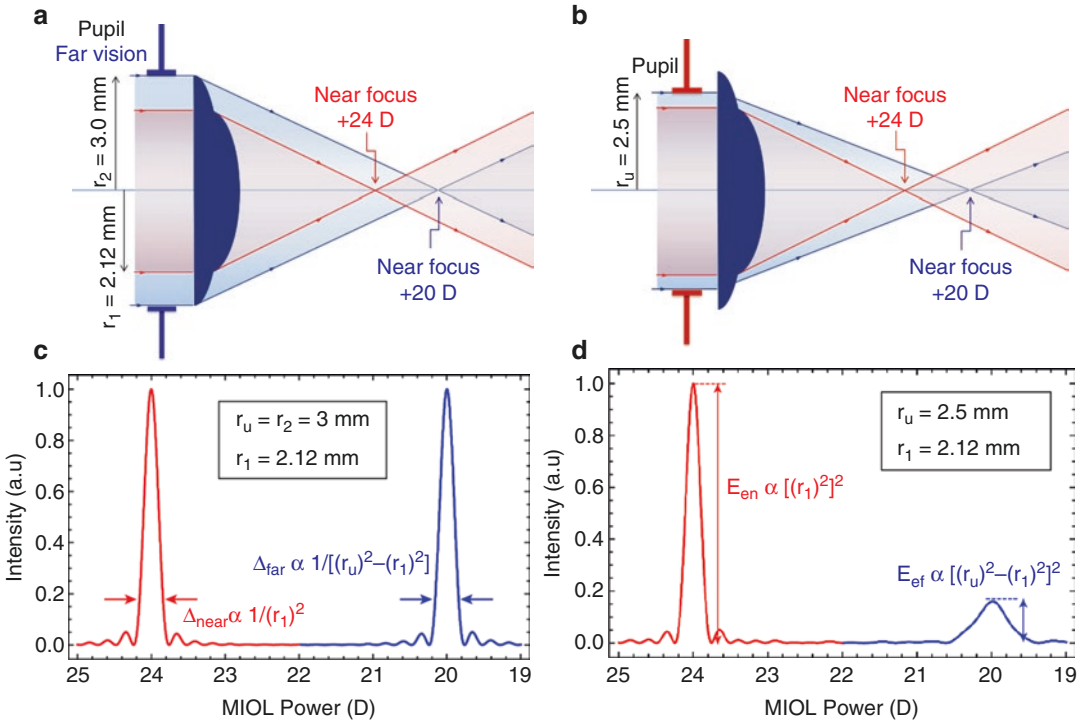


**Fig. 3.2** Light distribution and width of the focus in a refractive MIOL with  $P_{near} = 24$  D and  $P_{far} = 20$  D depending on the pupil size: (a) pupil size of 6 mm ( $r_u = 3$  mm),

(b) pupil size of 5 mm ( $r_u = 2.5$  mm), (c) light distribution for pupil size of 6 mm, (d) light distribution for pupil size of 5 mm

IOL is not good due to the rapid loss of the far focus, and other designs should be proposed to avoid this effect.

### 3.3 Diffractive Intraocular Lenses

Diffractive multifocal lenses have, instead of a flat surface, a multiscaled surface (named Fresnel surfaces or zones) that rises in concentric rings from the edge to the center. With this design several foci can be produced. Diffractive MIOLs are based on a monofocal refractive lens (called base lens) with different carved steps in one of the surfaces (Fig. 3.3c). The base lens produces a refraction of the wavefront focusing the light on the far focus (Fig. 3.3a). The diffractive pattern (Fig. 3.3b) is designed to enhance two principal foci (usually the 0 and first orders). The combination of both structures results in a multifocal

IOL whose powers are the sum of the base lens power plus the power of the diffractive orders (Fig. 3.3c).

Halos and glare will be also present in diffractive MIOL due to the energy expended in higher diffraction orders, scattering produced by the diffractive steps, and the residual level of aberrations (mainly SA) [3].

As commented above, in diffractive IOLs, concentric annular zones are created on the face of the lens. The emerging light from the various diffractive zones mixes and produces constructive interference at specific distances (called diffractive orders).

The limit of the  $j$ th zone occurs at a radius (Fig. 3.4):

$$r_j = \sqrt{2j\lambda_0 F} \quad (3.1)$$

where  $\lambda_0$  is the design wavelength and  $F$  is a design parameter that controls the position

**Fig. 3.3** Design of a diffractive MIOL: (a) refractive base lens of 20 D; (b) diffractive pattern with order 0 corresponding to infinite and order 1 to +4D; (c) diffractive MIOL with  $P_{near} = 24\text{ D}$  and  $P_{far} = 20\text{ D}$

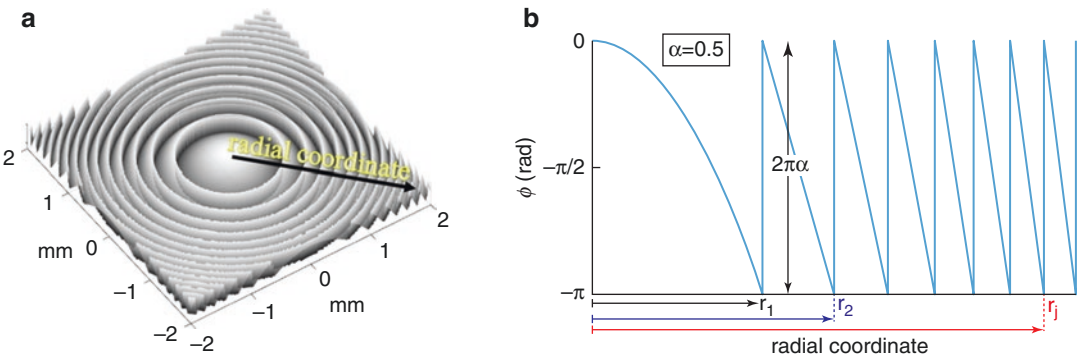
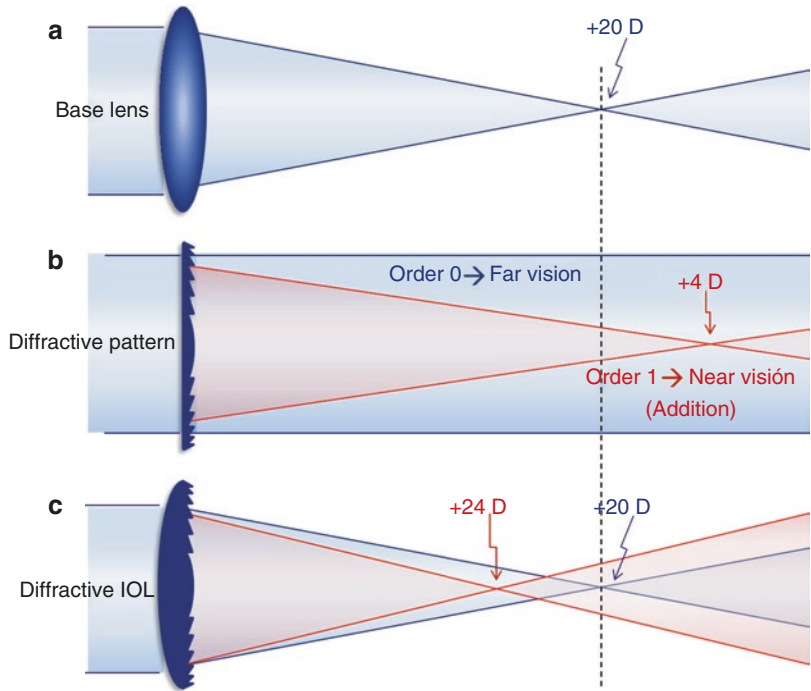


**Fig. 3.4** (a) Diffractive pattern and (b) phase profile generated by the diffractive pattern

of the generated foci. The  $m$  diffractive order will be located at the distance  $F/m$ . As can be deduced, the parameter  $F$  corresponds to the focal length of the first order, usually used as the add power.

The optical phase profile  $\phi(r)$  generated by the diffractive pattern, which is superimposed onto one of the base lens surfaces, modulates the phase of the corresponding emerging wave. This optical phase profile is given by [12]:

$$\phi(r) = 2\pi\alpha \left( j - \frac{r^2}{2\lambda_0 F} \right) r_j \leq r < r_{j+1} \quad (3.2)$$

where  $\alpha$  represents a fraction of the  $2\pi$  phase delay and is also a parameter of design that controls the relative energy that is sent to each focus.

Figure 3.4 represents both the pattern and the generated phase profile in a diffractive MIOL. As shown, the  $r_j$  radius determines the width of the steps and  $\alpha$  is directly related to the height of the steps.

From the expression of the phase ( $\phi(r)$ ) and using Fourier Optics, the following expression for the called diffraction energy efficiency ( $\eta$ ) has been already described<sup>10</sup>:

$$\eta_m = \sin^2 c^2(m - \alpha) \quad (3.3)$$

where  $m$  represents the diffraction order, the  $\sin c$  function (defined as  $\sin c(x) = \frac{\sin(\pi x)}{\pi x}$ ) dictates how the amount of emerging energy ( $E_e$ ) is distributed into each foci of focal  $F/m$ , and  $\eta_m$  indicates the percentage of light that reaches each focus. This distribution only depends on the parameter  $\alpha$  and therefore is independent from the pupil size. Notice that if  $\alpha = 1$ , the 100% of the light will reach the first order, and in consequence. The IOL will behave as a monofocal.

A typical diffractive multifocal IOL of 20 D and addition of +4 D can be achieved with these control parameters:  $\alpha = 0.5$  and  $F = 250$  mm (see Fig. 3.5). This configuration enhances two orders, specifically, the orders 0 and + 1. The dif-

fraction efficiency of the 0 order that corresponds

$$\text{to far vision } (P_{\text{far}} = P_{\text{base}} + P_{m=0} = 20 + \frac{0}{F} = 20 \text{ D})$$

is  $\eta_0 = 40.5\%$ . The diffraction efficiency of the +1 order that corresponds to near vision

$$(P_{\text{near}} = P_{\text{base}} + P_{m=+1} = 20 + \frac{1}{F} = 24 \text{ D}) \quad \text{is}$$

$\eta_{+1} = 40.5\%$  (see Fig. 3.5). The remaining 19% of the light energy is lost in other orders not desired. This configuration is popularly known as 50/50 distribution. However, this denomination can lead to confusion in the sense that it seems that 100% of the light that reaches the diffractive lens is equally distributed, but there is a loss of light (approximately 20%) that is destined to other non-desired foci.

In diffractive MIOLs, the percentage of light sent to each focus is independent from the pupil radius, but not from the total emerging light. Obviously, if the pupil size increases or decreases ( $r_u$  varies), the amount of energy will increase or decrease (see Fig. 3.5c, d). Furthermore,  $r_u$  will

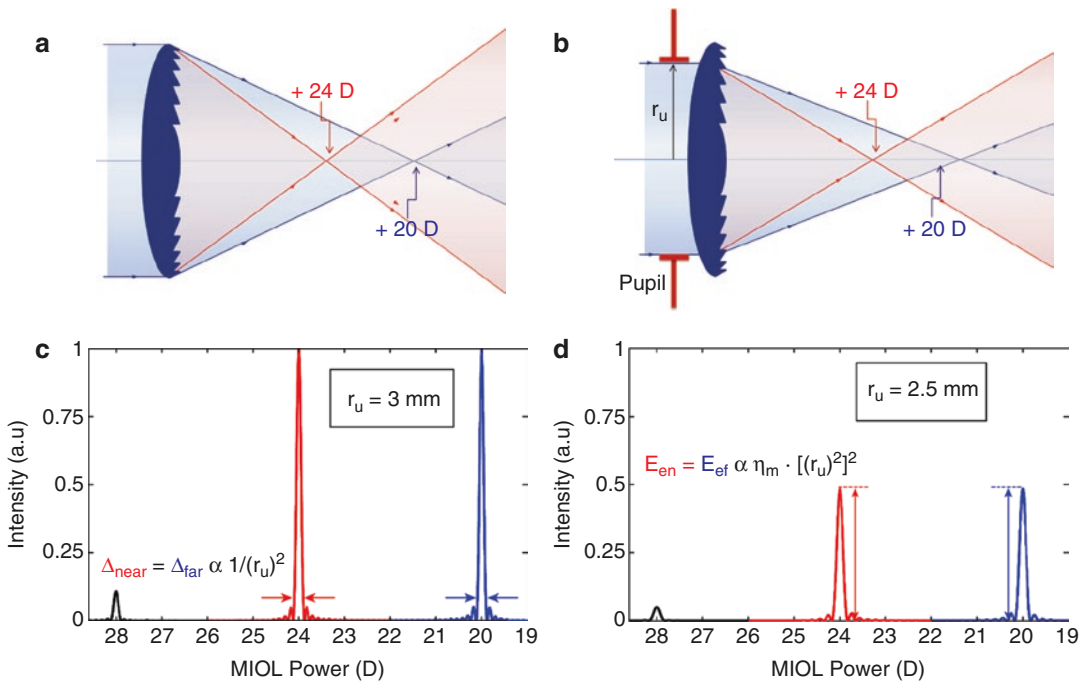


**Fig. 3.5** Light distribution and width of the focus in a diffractive MIOL with  $P_{\text{near}} = 24$  D and  $P_{\text{far}} = 20$  D depending on the pupil size: (a) pupil size of 6 mm ( $r_u = 3$  mm),

(b) pupil size of 5 mm ( $r_u = 2.5$  mm), (c) light distribution for pupil size of 6 mm, (d) light distribution for pupil size of 5 mm



equally determine the width and the energy of the foci. The width ( $\Delta$ ) of the foci depends on

$$\frac{1}{r_u^2}$$

each focus depends on  $\eta_m \cdot r_u^2$  (see Fig. 3.5c, d). This behavior is different from refractive MIOLs where the width and energy were different between foci.

Figure 3.5 shows an example of a diffractive MIOL with analogous characteristics ( $P_{\text{far}} = 20$  D and addition of +4 D) to that presented before in refractive MIOL format. The same pupil sizes of 6 mm and 5 mm have been also considered.

As it can be seen in Fig. 3.5c, d, diffractive MIOLs are always producing more than two foci corresponding to higher diffraction orders. In addition, when the useful radius ( $r_u$ ) decreases the emerging light ( $E_e$ ) is reduced (see Fig. 3.5d) but the percentage of light of each focus remains constant. Fig. 3.5c, d show the percentage is always of 40.5% independently of the pupil size. Furthermore, when  $r_u$  decreases, the width of

each focus increases, but it is the same in each focus (see Fig. 3.5c, d).

Only bifocal diffractive MIOLs have been mentioned, but also trifocal diffractive MIOL can be designed. The core of the trifocal design is based on the combination of two diffractive profiles in the same surface. These two diffractive profiles produce a serial of diffractive orders, some of which exactly provide the same focus. Combining the  $\alpha$  values of the two profiles ( $\alpha_1$  and  $\alpha_2$ ) appropriately, a specific light distribution can be achieved so that near, intermediate, and far foci are enhanced. For instance, the first pattern could produce a first-order diffraction that focuses on +4 D and therefore the second order on +8 D. In addition, the second diffraction pattern could provide a focus on +2 D and another one on +4 D. Thus, the focus of +4 D is common for both diffractive patterns (see Fig. 3.6).

The combination of these two diffractive patterns in the same surface will produce a phase variation as shown in Fig. 3.7, where  $\alpha_1 = 0.33$  and  $\alpha_2 = 0.33$  have been considered.

**Fig. 3.6** Explanation of how a trifocal diffractive lens can be obtained from two diffractive patterns that produce the overlapping of some orders

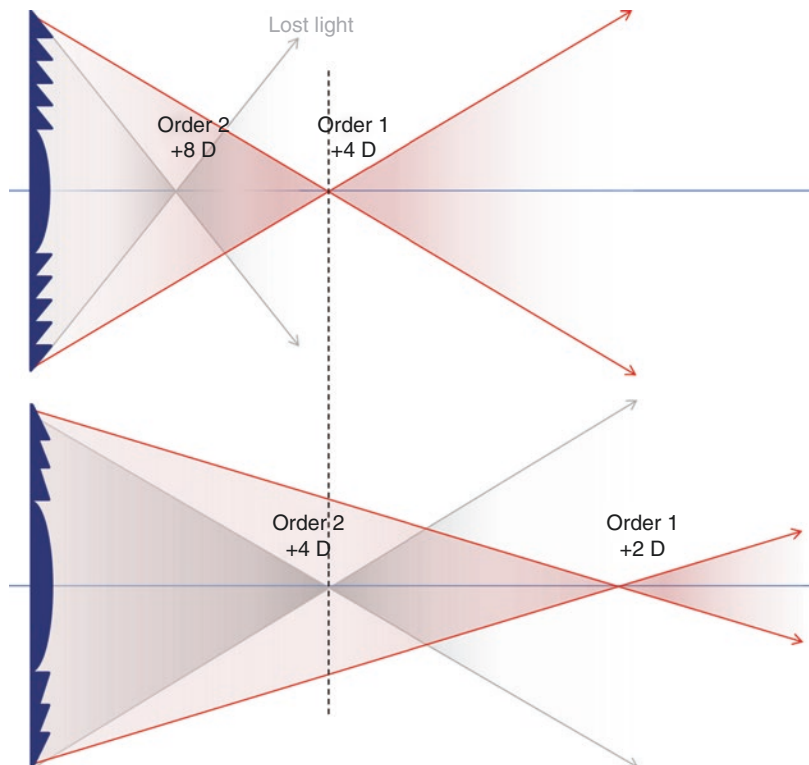


**Fig. 3.7** Phase profile of a trifocal diffractive MIOL when  $\alpha_1 = 0.33$  and  $\alpha_2 = 0.33$

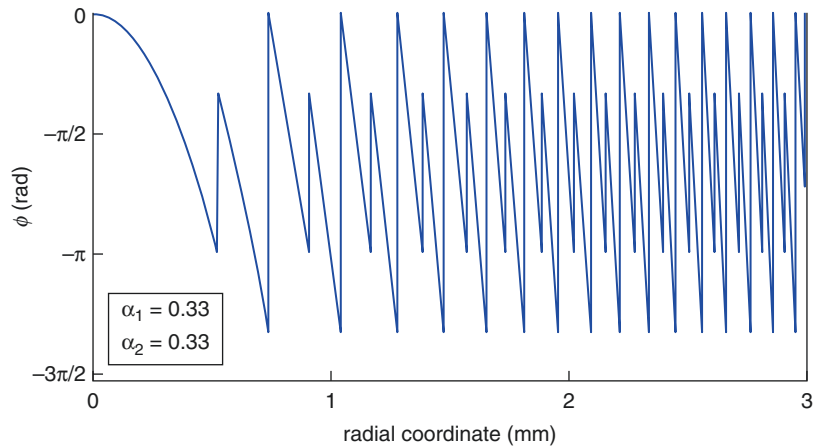
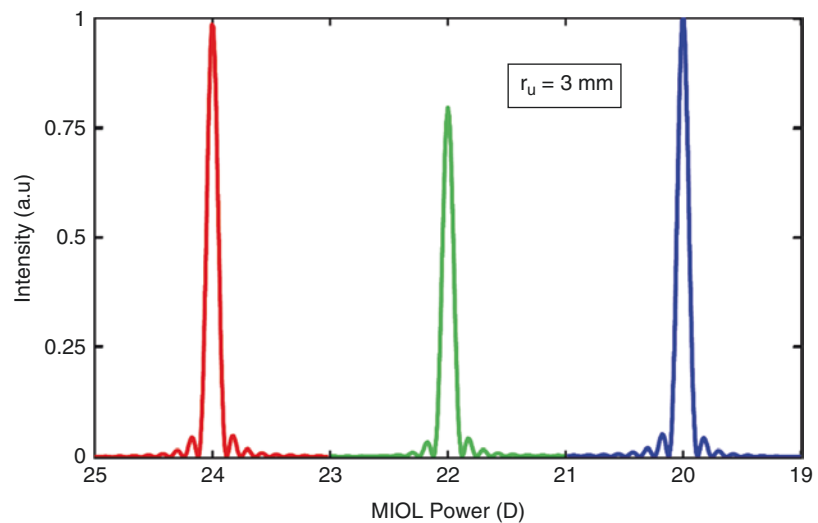


**Fig. 3.8** Light distribution of a trifocal MIOL



With this combination of two diffractive patterns, a trifocal diffractive MIOL with practically the same relative energy for each focus is obtained. In addition to a far focus, an intermediate focus of +2 D and a near focus of +4 D are obtained (see Fig. 3.8). Notice that as all diffractive IOLs, some amount of energy will be sent to not desired orders (see Fig. 3.6).

The light distribution correspondent to the phase variation of Fig. 3.7 is represented in Fig. 3.8. As it can be seen, the light is redistributed between three different foci. Far focus is receiving the highest energy and the intermediate focus the lowest energy. If it is assumed that the emerging light is about 80% (as it has been previously commented there is a loss of 20% of light), in

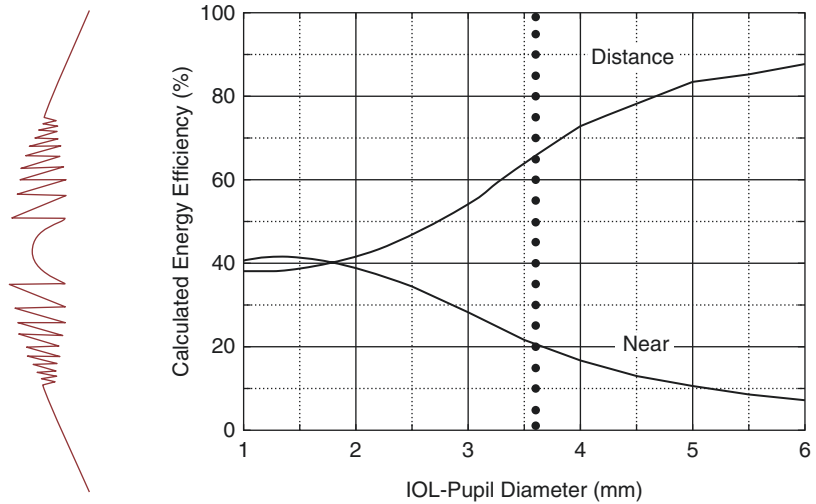
trifocal diffractive MIOLs this 80% is now redistributed in three foci whereas in the bifocal diffractive MIOLs this same amount of energy was redistributed in only two foci. Therefore, contrast sensibility and retinal illumination corresponding to some foci of the trifocal MIOLs will be worse compared to bifocal diffractive MIOLs.

### 3.3.1 Apodization

The apodization is an innovation in the diffractive lenses design of IOLs. This technique consists of designing the steps in such a way that the height decreases from the center of the optic toward its periphery. This variation produces a modula-



**Fig. 3.9** Example of a profile of a diffractive MIOL apodized (left) and the theoretical relative energy efficiency of the distance and near powers depending on the pupil size (right) [13]



tion of the phase profile and this implies that the parameter  $\alpha$  is now a function of the radial coordinate ( $\alpha(r)$ ). As a consequence, the percentage of relative energy in each focus becomes pupil dependent.

A typical variation of the energy efficiency depending on the pupil size of the apodized MIOLs is shown in Fig. 3.9. From this figure it can be understood that in scotopic conditions (larger pupil diameter), the periphery of the apodized diffractive optics acts. In the periphery the steps are lower and they send more energy to the far focus and less to the near one. The contrary occurs with myotic pupils, the near focus is energetically reinforced with respect to the far one.

### 3.3.2 Hybrid MIOLs

Another type of MIOLs are those that combine refractive and diffractive optics in the same surface. These types of MIOLs are called Hybrid Multifocal IOLs. Hybrid multifocal IOLs have a refractive basis, but in one surface there are two different zones: one diffractive and one refractive. Normally, the refractive zone contributes to the distance focus and the diffractive zone provides the addition, and also contributes to the far focus. The light distribution of these MIOLs is more complex because they share the characteristics of refractive and diffractive IOLs. With

respect to the diffractive zone, this will be clearly conditioned by the fact that there are a lower number of steps. Another important factor is that the area corresponding to the refractive area will be narrower and this will produce wider foci.

## 3.4 Extended Depth of Focus Intraocular Lens (EDOF IOLs)

Both refractive and diffractive MIOLs that have been described so far in previous sections provide two or three discrete foci. When only two foci are produced, the need of an additional focus is required for intermediate distance vision. This drawback was solved by trifocal MIOLs but accepting some loss of quality of vision in some foci. This loss is directly related to the light distribution because the emerging light must be divided into three foci instead of two. Consequently, less amount of light will reach each focus and a worsening of the contrast sensitivity and retinal illumination will be expected. In addition, a greater amount of photopic effects due to the greater number of existing jumps in the surface of the lens could be present. In this context, a new design of presbyopic-correcting IOLs emerges as a possible solution, the extended depth of focus IOLs (EDOF IOLs). The basic principle behind these lenses is to create a single-elongated focal point to enhance the depth of focus (DOF) or range of vision. This

elongated focus is meant to eliminate the overlapping of near and far images caused by traditional multifocal IOLs [14].

Depth of field is defined as the range of distance in which an object can be moved without the sharpness of the image falling below a tolerable level and the depth of focus (DOF) is defined as the conjugate interval in the image space. The level of visual tolerance is imposed by the visual system and will depend on each subject, although it varies little from one observer to another. This tolerance is related to the size of the maximum circle of tolerable blur for the visual system. The depth of focus of the human eye is basically a function of optical parameters (pupil size, optical aberrations, etc.) but is also affected by retinal, neural, and more complex psychophysical factors [15]. DOF has been demonstrated to depend on factors such as pupil size, Stiles–Crawford effect, ocular aberrations, and frequency of the stimulus or wavelength [16].

It is well known that modifying artificially the pupil size and some aberrations, the depth of focus of the eye can be modified. In the last decade, several MIOLs have used these characteristics in their designs to produce an enlargement of the depth of focus. The challenge of these MIOLs is to produce enough depth of focus to provide good vision for intermediate and near distances without a loss of quality of vision. In EDOF IOLs, the elongation of the focus is mainly obtained with two different methods: with the proper use and combination of aberrations or using the pinhole effect.

### 3.4.1 Use of Aberrations

Some studies have evaluated the effect of the addition of spherical aberration or coma in the enlargement of DOF. For pupil sizes between 3 mm and 6 mm, increments between 0.4 D and 0.7 D approximately can be produced with the addition of 0.3  $\mu\text{m}$  or 0.6  $\mu\text{m}$  of negative spherical aberration respectively [17]. Furthermore, the effect of coma has been also analyzed. The increment of DOF using vertical coma can range between 0.3 D and 0.8 D depending

on the studies [18]. Combination of 0.4  $\mu\text{m}$  of fourth-order spherical aberration and 0.2  $\mu\text{m}$  of sixth-order spherical aberration of opposite signs has been also proposed to induce a bimodality in the through-focus curve second peak that can produce an enlargement of the depth of focus [18–20].

The use of negative spherical aberration has been used in both monofocal and multifocal IOLs for many years. These lenses with negative spherical aberration try to simulate the negative spherical aberration of the crystalline lens, but there is also an enlargement of the focus at the same time. The optics of the EDOF IOLs used to be hybrid, combining an external refractive zone for far vision and internal diffractive zone for far and intermediate vision. For instance, the Symphony IOL (Tecnis, Abbott Medical Optics Inc., Johnson and Johnson vision) combines a unique diffractive pattern with achromatic technology and a proprietary echelette design resulting in an elongated depth of focus.

Recently, a new type of purely refractive EDOF IOL based on combinations of spherical aberrations has appeared (Mini Well Ready of SIFI). Considering that refractive lenses can already produce wider focal points, this EDOF IOL uses wavefront technology to enhance range of vision, combining negative primary and positive spherical aberrations [10, 21]. The IOL has three circular zones, each with a different aspheric profile: a central zone inducing positive spherical aberration, an intermediate zone inducing negative spherical aberration, and an aspheric monofocal zone in the periphery (Fig. 3.10). The combination of spherical aberrations of different sign is producing an enlargement of the focus as it can be seen in Fig. 3.10b.

Two important factors that should be considered when the aberrations are used in EDOF IOLs are the interaction with the pre-existing corneal aberrations and the centering of the IOL-eye system. These effects have not been widely analyzed and they are likely to influence the final clinical results. To date, only few studies have been carried out to trying to predict the effect of the interaction between ocular and EDOF IOLs aberrations [10, 21].

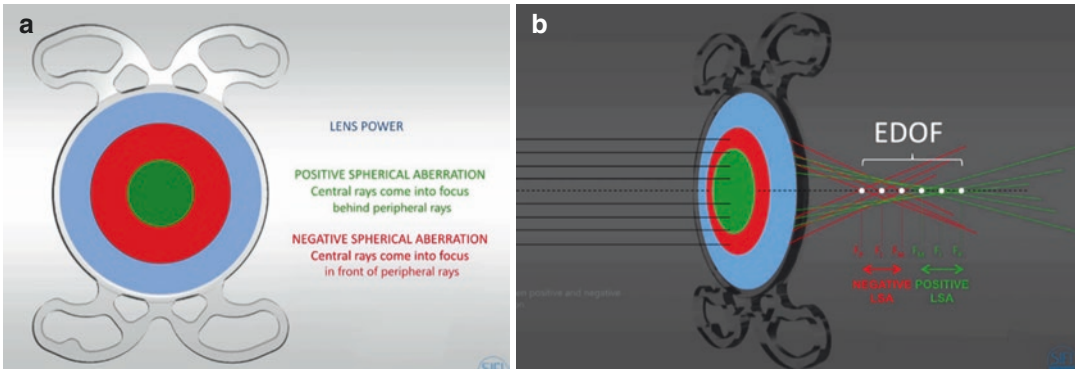


**Fig. 3.10** (a) Design of combination of primary and secondary spherical aberration; (b) Depth of focus produced by the combination of the positive and negative spherical aberrations

### 3.4.2 Pinhole Effect

In the 1960s, Campbell experimentally determined the value of depth of field in the eye and found the following empirical relationship [22]:

$$DOF = \frac{0.75}{\phi_{EP}} + 0.08(D) \quad (3.4)$$

where  $\phi_{EP}$  is the diameter of the entrance pupil in mm.

In paraxial optics, this expression is equivalent in diopters for the depth of focus. From this equation, it can be deduced that the higher the pupil size is, the lower the depth of field is and consequently the depth of focus. Following this principle, the use of an opaque mask pinhole incrustated in a monofocal IOL could produce the pinhole effect and enhance the depth of focus. In this type of EDOF IOLs, there is an important loss of light due to the opaque mask which is proportional to its area. The emerging light from these EDOF IOLs will come from the transparent zone and the light distribution along the axis will depend on the size of the pinhole. An example of an EDOF IOL based on this concept is the IC-8 IOL. This IOL incorporates a non-diffractive 3.23 mm diameter opaque mask with a 1.36 mm central aperture embedded within a 6.0 mm one-piece hydrophobic acrylic lens. Applying the

Eq. 3.4, an estimation of the depth of field produced in the eye by this aperture can be done:

$$DOF = \frac{0.75}{1.36} + 0.08 = 0.63 \text{ D}$$

This DOF could be enlarged due to the wider focus provided by the refractive IOL as well as if it is combined with spherical aberration, although the interaction between aberrations and pupil size is not clear [23].

In conclusion, in EDOF IOLs there is a compromise between visual quality and distance vision, since there is a loss of visual quality (more aberrations or less retinal illumination) in exchange for increasing the range of distances that can be seen with sufficient quality. The worsening of the visual quality is due to the loss of the contrast sensitivity since from a theoretical point of view the generation of a greater depth of focus implies a worsening of the PSF of the system or a decrease of the MTF. Therefore, the advantages or disadvantages of different EDOF are not easy to establish, and they will depend on the refractive or diffractive nature of the IOL and its design.

#### Compliance with Ethical Requirements

**Conflicts of Interest** The authors have no proprietary or commercial interest in the medical devices that are involved in this manuscript.

**Informed Consent** This chapter does not show the results of studies involving human or animal subjects.

**Funding** Author David P Piñero has been supported by the Ministry of Economy, Industry and Competitiveness of Spain within the program Ramón y Cajal, RYC-2016-20471.

## References

- de Gracia P, Dorronsoro C, Sánchez-González Á, Sawides L, Marcos S. Experimental simulation of simultaneous vision. *Invest Ophthalmol Vis Sci*. 2013;54(1):415–22.
- Alio JL, Plaza-Puche AB, Fernandez-Buenaga R, Pikkell J, Maldonado M. Multifocal intraocular lenses: an overview. *Surv Ophthalmol*. 2017;62(5):611–34. <https://doi.org/10.1016/j.survophthal.2017.03.005>.
- Vega F, Alba-Bueno F, Millan MS, Varon C, Gil MA, Buil JA. Halo and through-focus performance of four diffractive multifocal intraocular lenses. *Invest Ophthalmol Vis Sci*. 2015;56(6):3967–75. <https://doi.org/10.1167/iovs.15-16600>.
- Vega F, Millan MS, Vila-Terricabras N, Alba-Bueno F. Visible versus near-infrared optical performance of diffractive multifocal intraocular lenses. *Invest Ophthalmol Vis Sci*. 2015;56(12):7345–51. <https://doi.org/10.1167/iovs.15-17664>.
- Castignoles F, Flury M, Lepine T. Comparison of the efficiency, MTF and chromatic properties of four diffractive bifocal intraocular lens designs. *Opt Express*. 2010;18(5):5245–56.
- Flores A, Wang MR, Yang JJ. Achromatic hybrid refractive-diffractive lens with extended depth of focus. *Appl Optics*. 2004;43(30):5618–30.
- Hoffer KJ, Savini G. Multifocal intraocular lenses: historical perspective. In: *Multifocal intraocular lenses*: Springer; 2014. p. 5–28.
- Davison JA, Simpson MJ. History and development of the apodized diffractive intraocular lens. *J Cataract Refract Surg*. 2006;32(5):849–58. <https://doi.org/10.1016/j.jcrs.2006.02.006>.
- Schwiegerling J. Intraocular lenses. In: Bass MVS, WWilliams E, Wolfe DR, William L, editors. *Handbook of optics. Vision and vision optics*, vol. 3. New York: McGraw-Hill; 2010. p. 21–7.
- Camps VJ, Tolosa A, Pinero DP, de Fez D, Caballero MT, Miret JJ. In vitro aberrometric assessment of a multifocal intraocular lens and two extended depth of focus IOLs. *J Ophthalmol*. 2017;2017:7095734. <https://doi.org/10.1155/2017/7095734>.
- Zeng L, Fang F. Advances and challenges of intraocular lens design [invited]. *Appl Optics*. 2018;57(25):7363–76. <https://doi.org/10.1364/AO.57.007363>.
- Faklis D, Morris GM. Spectral properties of multiorder diffractive lenses. *Appl Optics*. 1995;34(14):2462–8. <https://doi.org/10.1364/AO.34.002462>.
- Vega Lerín F, Alba Bueno F, Millán Garcia-Varela MS. Energy distribution between distance and near images in apodized diffractive multifocal intraocular lenses. *Invest Ophthalmol Vis Sci*. 2011;52(8):5695–701.
- Akella SS, Juthani VV. Extended depth of focus intraocular lenses for presbyopia. *Curr Opin Ophthalmol*. 2018;29(4):318–22. <https://doi.org/10.1097/ICU.0000000000000490>.
- Green DG, Powers MK, Banks MS. Depth of focus, eye size and visual acuity. *Vision Res*. 1980;20(10):827–35. [https://doi.org/10.1016/0042-6989\(80\)90063-2](https://doi.org/10.1016/0042-6989(80)90063-2).
- Marcos S, Moreno E, Navarro R. The depth-of-field of the human eye from objective and subjective measurements. *Vision Res*. 1999;39(12):2039–49.
- Benard Y, Lopez-Gil N, Legras R. Subjective depth of field in presence of 4th-order and 6th-order zernike spherical aberration using adaptive optics technology. *J Cataract Refract Surg*. 2010;36(12):2129–38.
- Legras R, Benard Y, Lopez-Gil N. Effect of coma and spherical aberration on depth-of-focus measured using adaptive optics and computationally blurred images. *J Cataract Refract Surg*. 2012;38(3):458–69.
- Benard Y, Lopez-Gil N, Legras R. Optimizing the subjective depth-of-focus with combinations of fourth- and sixth-order spherical aberration. *Vision Res*. 2011;51(23–24):2471–7.
- Yi F, Iskander DR, Collins M. Depth of focus and visual acuity with primary and secondary spherical aberration. *Vision Res*. 2011;51(14):1648–58.
- Camps VJ, Miret JJ, Garcia C, Tolosa A, Pinero DP. Simulation of the effect of different presbyopia-correcting intraocular lenses with eyes with previous laser refractive surgery. *J Refract Surg*. 2018;34(4):222–7. <https://doi.org/10.3928/1081597X-20180130-02>.
- Campbell FW. The depth of field of the human eye. *Opt Acta*. 1957;4(4):157–64.
- Marcos S, Moreno E, Navarro R. The depth-of-field of the human eye from objective and subjective measurements. *Vision Res*. 1999;39(12):2039–49.